Memorias del Congreso Nacional de Control Automático
ISSN: 2594-2492

Fault Pattern Recognition for Pipelines with Viscous Fluid ⋆

Jesús Peralta * **Cristina Verde** *

* *Instituto de Ingeniería Universidad Nacional Autónoma de México, 04510, CDMX, México (e-mail: jealperalta@gmail.com, verde@unam.mx)*

Abstract: This paper deals with the detection and localization of damage in pipelines. The purpose is to characterize the transient wave propagation in a faulty pipeline with a viscous absorption fluid and the pattern response to an external acoustic source as a function of the fault type and position. The study assumes an infinite-dimensional linear model for the wave propagation in the pipeline and lumped models for the leak and blockage faults. The key to the study is to analyze the wave propagation model through graph theory and by the reflection coefficient to solve these tasks. The system decomposition according to the fault scenarios allows the characterization of the impulse input response for a leak and blockage in the pipeline. For the specific case of a leak and a blockage, the impulse patterns are established and validated by simulation.

Keywords: Feature selection for fault location, signal patterns for leak and blockage detection, signal graph theory.

1. INTRODUCTION

Pipelines and distribution networks are the most common and economical way to transport fluids. The number of pipelines around the world and the fact that the products are mainly hazardous demand norms and requirements from government and society for safe installations (Farmer, 2017; Lu and Iseley, 2018). The main reason for the pipelines system (PS) degradation is the destruction of pipe walls as a result of corrosion, erosion, fatigue damage accumulation, static and shock loading, frost upheaval, ice load, turbulent flows, and so on. The main concern of the utilities and distributers of liquid and gas is the diagnosis of leakage since it results not only in product loss but also generates accidents with huge potential damage.

Recently, Murvay and Silea as well as Datta and Sarkar (2016) published a very exhaustive review of different methods for PS fault diagnosis based on the applicability of the methods that included the vibration analysis, pulse echo methodology, acoustic techniques, negative pressure wave, artificial intelligence tools, interferometric optic, and so on. The acoustic pulse reflectometry principle is suggested as the more suitable because of its proficiency in identifying both blockage and leakage in a pipe.

According to Sattar and Chaudhry (2008), the multiple leaks' problem can be tackled in the frequency domain with linearized models of the fluid and by assuming punctual faults. The transient test-based tools are considered useful for leak and blockage detection in a line as is shown in Meniconi et al. (2016) and Capponi et al. (2017). Thus, the transient oscillatory pressure produced by the source allows detecting faults in the time (Rubio Scola et al., 2015) and frequency domain (Mpesha et al., 2001).

Since the excitation signal produced by a valve is not always feasible in a line for security reasons, the idea of replacing the oscillating valve with acoustic signals injected into the line has been also proposed in diverse contributions. A change in the impedance of the fluid is produced by a fault in the conduit (Sharp and Campbell, 1997). As a consequence, an acoustic source can be used as perturbation, and the reflection phenomenon allows the identification of the fault. Thus, the authors proposed an external acoustic signal injected into the pipeline to detect the damage conditions by means of information collected at the measurement point.

Motivated by the facts mentioned above, this work focuses on two tasks: looking for the transient wave propagation properties in a damaged pipeline with a viscous fluid and pattern responses as a function of the damage type and its location. In particular, by taking advantage of the graph theory, a study is proposed that joins an infinite-dimensional linear model of the wave propagation together with its analysis through graph theory to solve these tasks. The assumed faults in the study are a leak

⋆ This work is supported by IT100519-DGAPA-UNAM and 280170conv2016-3 SENER-CONACyT.

Copyright©AMCA. Todos los Derechos Reservados www.amca.mx

and a discrete blockage modeled as components of lumped parameters.

Consider the setup system of Fig. 1. The first part of this work introduces the analytical infinite-dimensional linear model of the fluid in the complex domain with a single fault by assuming an injection of a acoustic signal at the upstream boundary of the line and with a single measurement point of the wave pressure at distance l_0 from the source. The system model is developed by using two-port transfer matrices that are coupled with algebraic operations according to the fault and boundary conditions.

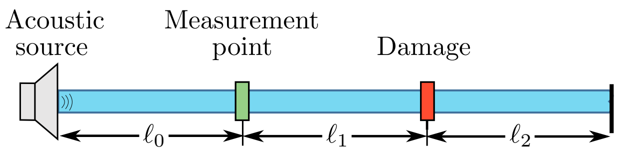

Figure 1. Sketch of an interconnected pipe with three healthy segments, a fault, measurement point and an acoustic source as a test signal

The whole system in fault conditions as oriented subgraphs considering an impulse as an acoustic signal allows analyzing the wave propagation trajectories in the time domain based on the paths described by the graphs. This analysis simplifies the search for the fault parameters in the impulse propagation and allows the recognition of a specific pattern in the response for each type of fault. This idea is the main contribution of this work. The fault position is associated with the arrival time of the first reflected wave at the measurement point, and the amplitude of the reflected wave characterizes the type and magnitude of the fault. Section 5 validates the proposed impulse response patterns for the faults in diverse conditions through simulation, and, finally, Section 6 includes the main conclusions and remarks. The main advantage of the proposed detection test is the straightforward interpretation of the parameters associated with each fault and its generalization for a combination of multiple faults. Moreover, from a practical point of view, the test requires only an external acoustic source and a measurement point of transient pressure for the fault identification.

2. SYSTEM STRUCTURE AND WAVE PROPAGATION MODEL

In order to analyze the system shown in Fig. 1, this section introduces the propagation model of acoustic waves with attenuation because of viscosity and faults. The system configuration consists of the following: three healthy conduit segments interconnected with two lumped parameter components and boundary conditions at the ends of the conduit. The first component named *measurement point* is where the state of the acoustic wave is measured and recorded. The second one represents a fault in a point of the conduit that could be a leakage or a partial blockage. The healthy conduit segments are modeled by a two-port transfer matrix, which relates the acoustic pressure and particle velocity at its ends.

2.1 Intact Pipeline Model

The propagation equations of acoustic waves through a pipe of a constant of cross-section area S [m^2] and length ℓ [m] can be derived from the continuity, momentum and the gas state equations governing the dynamics of the fluid considering absorption caused by viscosity. According to Blackstock (2000), these equations can be expressed as a set of linearized one-dimensional partial differential equations as follows:

$$\frac{\partial \rho(z,t)}{\partial t} + \rho_0 \frac{\partial u(z,t)}{\partial z} = 0, \tag{1}$$

$$\rho_0 \frac{\partial u(z,t)}{\partial t} + \frac{\partial p(z,t)}{\partial z} = \eta \frac{\partial^2 u(z,t)}{\partial z^2}, \tag{2}$$

$$p(z,t) = c^2 \rho(z,t), \tag{3}$$

where $(z,t) \in [0,\ell] \times [0,+\infty)$ gathers the space [m] and time [s] coordinates and $p(z,t)$, $u(z,t)$ and $\rho(z,t)$ denote the acoustic pressure [Pa], the particle velocity [m/s] and the medium density variations [kg/m^3], respectively. Furthermore, ρ_0 is the medium density at the operation point, c is the sound speed in the fluid [m/s] and η gathers the coefficients associated with the viscosity of the fluid [Pa·s].

To obtain the wave equation for a segment, the density $\rho(z,t)$ given in (3) is substituted in (1), and one gets

$$\frac{1}{c^2}\frac{\partial p(z,t)}{\partial t} + \rho_0 \frac{\partial u(z,t)}{\partial z} = 0. \tag{4}$$

Thus, by taking the partial derivatives of (4) and (2) with respect to z and t, after some algebraic manipulations the particle velocity model can be written by

$$\frac{\partial^2 u(z,t)}{\partial z^2} + \frac{\eta}{\rho_0 c^2}\frac{\partial^3 u(z,t)}{\partial z^2 \partial t} - \frac{1}{c^2}\frac{\partial^2 u(z,t)}{\partial t^2} = 0. \tag{5}$$

By transforming this equation into the frequency domain s, the wave velocity propagation model is reduced to

$$\frac{d^2 U(z,s)}{dz^2} - \gamma^2(s) U(z,s) = 0, \tag{6}$$

where the propagation function is given by

$$\gamma(s) = \frac{1}{c}\frac{s}{\sqrt{1+\delta_v s}} = \frac{\tilde{\gamma}(s)}{c}, \tag{7}$$

with $\delta_v = \eta/\rho_0 c^2$ [s]. Thus, the solution of (6) takes the form

$$U(z,s) = c_1(s)\sinh\left(\tilde{\gamma}(s)\frac{z}{c}\right) + c_2(s)\cosh\left(\tilde{\gamma}(s)\frac{z}{c}\right), \tag{8}$$

where $c_1(s)$ and $c_2(s)$ are functions of s determined by the segment boundary conditions.

On the other hand, by transforming (4) into the frequency domain, one gets the acoustic pressure

$$\frac{s}{c^2}P(z,s) + \rho_0 \frac{dU(z,s)}{dz} = 0, \tag{9}$$

as a function of the derivative of the velocity. Since $U(z,s)$ is given by (8), one can substitute its derivative in (9) to obtain the expression of the acoustic pressure

 Copyright©AMCA. Todos los Derechos Reservados www.amca.mx

$$P(z,s) = -Z(s)\left(c_1(s)\cosh\left(\tilde{\gamma}(s)\frac{z}{c}\right) + c_2(s)\sinh\left(\tilde{\gamma}(s)\frac{z}{c}\right)\right) \tag{10}$$

with $Z(s) = \rho_0 c\tilde{\gamma}(s)/s$ as the acoustic impedance. Thus, by defining the state at the ends with any arbitrary boundary as

$$X(z^-,s) = \begin{bmatrix} P(z^-,s) \\ U(z^-,s) \end{bmatrix} \text{ and } X(z^+,s) = \begin{bmatrix} P(z^+,s) \\ U(z^+,s) \end{bmatrix}, \tag{11}$$

the functions $c_1(s)$ and $c_2(s)$ can be determined by

$$c_1(s) = -\frac{1}{Z(s)}P(z^-,s) \text{ and } c_2(s) = U(z^-,s). \tag{12}$$

Therefore, the wave state at the ends is related to

$$X(z^+,s) = M^\ell(s)X(z^-,s), \tag{13}$$

where $z^+ - z^- = \ell$ and the transfer matrix

$$M^\ell(s) = \begin{bmatrix} \cosh\left(\tilde{\gamma}(s)\frac{\ell}{c}\right) & -Z(s)\sinh\left(\tilde{\gamma}(s)\frac{\ell}{c}\right) \\ -\frac{1}{Z(s)}\sinh\left(\tilde{\gamma}(s)\frac{\ell}{c}\right) & \cosh\left(\tilde{\gamma}(s)\frac{\ell}{c}\right) \end{bmatrix} \tag{14}$$

corresponds to the two-port model for an intact segment of length ℓ (Chaudhry, 2013). This model is used to describe any of the three segments of the tube shown in Fig. 1 with the same propagation function $\gamma(s)$, impedance $Z(s)$ and their respective lengths. The algebraic form of the matrix $M^\ell(s)$ differs from the wave models reported in Lee et al. (2005) as well as Wang et al. (2021) in the propagation function.

2.2 Components Lumped Models

According to Chaudhry (2013), a point component at point z_k in a conduit produces a discontinuity. In the framework of two ports, such a component is modeled as a transfer matrix that depends on the specific component that relates to the fluid state X before and after the component. This is

$$X(z_k^+,s) = \mathcal{P}^{z_k}(s)X(z_k^-,s), \tag{15}$$

where $z_k^+ = z_k + \epsilon$, and $z_k^- = z_k - \epsilon$ are space coordinates close to z_k, with $\epsilon \to 0$ and the matrix $\mathcal{P}^{z_k}(s)$ relates to the upstream and downstream states of the component. The following paragraphs introduce the point transfer matrices for two types of faults: a leakage and a partial blockage.

Leakage Model: The discharge produced by a leak at point z_k in a pipeline with cross-section area S can be described by the two-port lumped model

$$X(z_k^+,s) = \mathcal{P}_l^{z_k}X(z_k^-,s) \text{ with } \mathcal{P}_l^{z_k} = \begin{bmatrix} 1 & 0 \\ -(F_l^*S)^{-1} & 1 \end{bmatrix} \tag{16}$$

taken from Zecchin et al. (2005), which depicts the deviations upstream and downstream from the steady-state wave near point z_k, with the leak impedance $F_l^* = 2p_l/q_l$ [Pa·s/m^3] as the ratio of the steady-state discharge through the orifice q_l [m^3/s] to the respective pressure p_l [Pa] in the leak.

Based on reflectometry, when a wave traveling through the duct falls on a leak, the impedance F_l^* produces reflected waves in the line that are characterized by the coefficients of the dimensionless reflection $R_l(s)$ and transmission $T_l(s)$. These coefficients are written in terms of the leak and acoustic impedances F_l^* and $Z(s)$ as reported in Zecchin et al. (2005):

$$R_l(s) = -\frac{Z(s)}{2F_l^*S + Z(s)} \text{ and } T_l(s) = \frac{2F_l^*S}{2F_l^*S + Z(s)} \tag{17}$$

with $T_l(s) = 1 + R_l(s)$.

Partial Blockage Model: Following a similar derivation as for the leak scenario, the following reflection and transmission coefficients $R_b(s)$ and $T_b(s)$ can be obtained:

$$R_b(s) = \frac{F_b^*S}{2Z(s) + F_b^*S} \text{ and } T_b(s) = \frac{2Z(s)}{2Z(s) + F_b^*S}, \tag{18}$$

in terms of the blockage impedance $F_b^* = 2\Delta p_0/q_0$ [Pa·s /m^3]. F_b^* is associated with the partial blockage that depends on the steady-state pressure loss across the valve Δp_0 [Pa] corresponding to the steady-state of the flow rate q_0 [m^3/s]. Here $T_b(s) = 1 - R_b(s)$. Thus, the partial blockage lumped model is written as

$$X(z_k^+,s) = \mathcal{P}_b^{z_k}X(z_k^-,s) \text{ with } \mathcal{P}_b^{z_k} = \begin{bmatrix} 1 & -F_b^*S \\ 0 & 1 \end{bmatrix}. \tag{19}$$

As a result, based on the above developed transfer matrices and the features of the device components, one can already obtain the global model of an acoustic wave for the configuration shown in Fig. 1. The analytical model that links the state $X(z,s)$ along the pipe by interconnecting the components according to the configuration is developed in Subsection 2.4.

2.3 Frequency Response of Reflection Coefficients to Different Gas Propagation Mediums

The reflection coefficients given by (17) and (18) are an important object in the study of fault detection because they represent a magnitude of energy loss from the incident acoustic wave. Thus, it is important to perform a study on frequency response. The magnitude diagram of $R_l(s)$ depicted by Fig. 2 shows that for low frequencies' signals the gain obtained for different gaseous propagation mediums like air, O_2, N_2 and CO_2 are constants with values of $F_l^* = 98,100$ and $F_b^* = 784,800$ Pa $\cdot$ s/m^3. A similar event occurs with $R_b(s)$.

Thus, it is possible to analyze the fault models considering that the reflection coefficients are constant values: they do not depend on variable s. Moreover, since the relationships between the reflection and transmission coefficients are linear, they can also be considered as constants. Furthermore, the reflections coefficients can be approximated as

$$R_l \approx -\frac{\rho_0 c}{2F_l^*S + \rho_0 c} \text{ and } R_b \approx \frac{F_b^*S}{2\rho_0 c + F_b^*S}. \tag{20}$$

If a specific means of propagation through a pipeline is considered, the above equations imply static relationships

 Copyright©AMCA. Todos los Derechos Reservados www.amca.mx

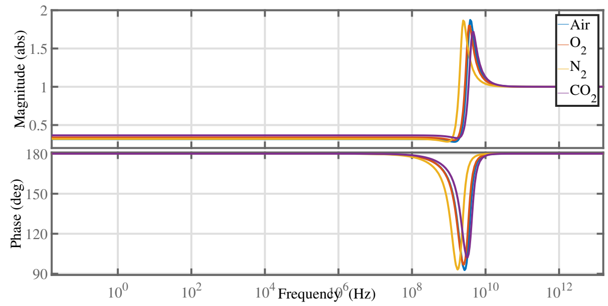

Figure 2. Gain and phase of function $R_l(s)$ for different propagation mediums at 20°C

between the reflection coefficients and the associated impedances for each of the faults. Therefore, by making an identification of the parameter R_f, it is possible to identify the parameter F_f^* that allows estimating the magnitude of the fault. These relations are depicted by Figs. 3 and 4.

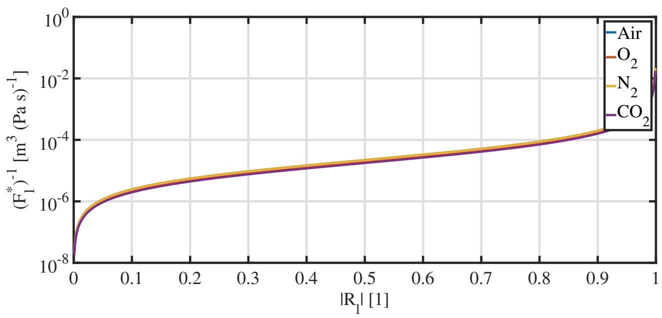

Figure 3. Relationship between $|R_l|$ and the inverse of F_l^*

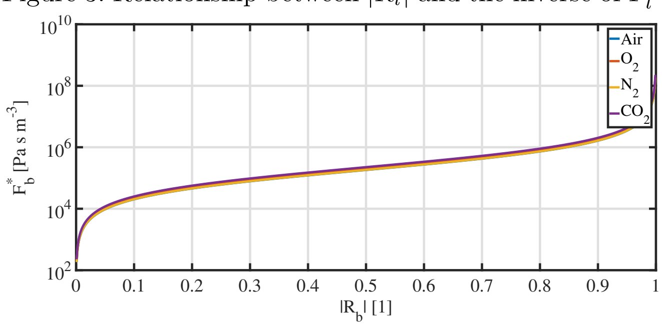

Figure 4. Relationship between $|R_b|$ and F_b^*

As a result, on the basis of the transfer matrices developed above and the analysis of the frequency response of the reflection coefficients, one can already obtain the global model of an acoustic wave traveling for the configuration shown in Fig. 1 by considering that the reflection coefficients are constants. The analytical model that links the state $X(z, s)$ along the pipe by interconnecting the components according to the configuration is developed in the next subsection.

2.4 Embedded Model

The block diagrams of Fig. 5 give a description of the whole system where $X(0)$ is associated with the excitation source and $X(L)$ with the condition at the end of the line of length L. Hereafter the dependency on s is omitted for simplicity, and the set of matrices $\{M^{\ell_0}, M^{\ell_1}, M^{\ell_2}\}$ is associated with (14) for the intact sections of lengths ℓ_0, ℓ_1, and ℓ_2, respectively. These lengths satisfy $L = \ell_0 + \ell_1 + \ell_2$. The unit matrix $\mathcal{P}_o^{z_0}$ associated with the point z_0 is where the state can be observed and recorded, as well as the matrix $\mathcal{P}_f^{z_1}$ associated with a fault at coordinate $z_1 = \ell_0 + \ell_1$, where the subindex $f = l$ or b denotes if the fault is a leak or a partial blockage, respectively.

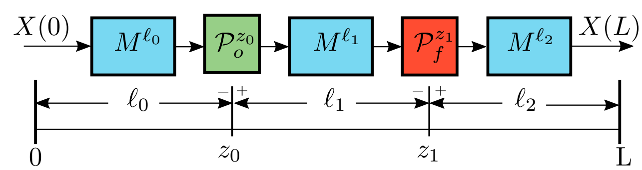

Figure 5. Matrix block diagram of the acoustic system with a fault at z_1 and an observation point at z_0

Because $\mathcal{P}_o^{z_0} = I$ for the wave state at the observation point, one can write the relation

$$X(z_0) = M^{\ell_0} X(0), \tag{21}$$

and for the state at the end of the line in terms of $X(z_0)$, one can also write the relation

$$X(L) = \mathcal{S}^{\ell_2,\ell_1} X(z_0) \text{ with } \mathcal{S}^{\ell_2,\ell_1} = M^{\ell_2} \mathcal{P}_f^{z_1} M^{\ell_1}. \tag{22}$$

Thus, from (21) and (22), the state at the observation point can be expressed in terms of the boundary conditions by

$$X(z_0) = \frac{1}{2}\left(M^{\ell_0} X(0) + \left(\mathcal{S}^{\ell_2,\ell_1}\right)^{-1} X(L)\right), \tag{23}$$

which depends on the transfer matrix between the observation point and the fault, as well as the transfer matrix between the fault and the end of the pipeline.

On the other hand, the transfer matrix between the boundary conditions at the ends of the pipe can be expressed by

$$X(L) = TX(0) \text{ with } T = \begin{bmatrix} t_{11} & t_{12} \\ t_{21} & t_{22} \end{bmatrix} = \mathcal{S}^{\ell_2,\ell_1} M^{\ell_0}. \tag{24}$$

These relations are valid for any excitation source and downstream condition, as well as for any type of fault with a punctual matrix model. Moreover, this is straightforwardly extended for the case of two faults in the line.

3. WAVE BEHAVIOR AT THE MEASUREMENT POINT

To analyze the wave behavior at the measurement point z_0 under fault scenarios, specific boundary conditions $X(0)$ and $X(L)$ must be given in (23). Upstream pressure

 Copyright©AMCA. Todos los Derechos Reservados www.amca.mx

$X_1(0) = P(0)$ is assumed to be the excitation source signal in the pipe, and the downstream velocity $X_2(L) = 0$ is assumed to be the boundary condition produced by a rigid body. $X_1(0)$ and $X_1(L)$ are obtained directly from (24). In this way, the boundary conditions can be written as a function of the external source $P(0)$ as

$$X(0) = \begin{bmatrix} 1 \\ -\frac{t_{21}}{t_{22}} \end{bmatrix} P(0), \quad X(L) = \begin{bmatrix} \frac{1}{t_{22}} \\ 0 \end{bmatrix} P(0). \tag{25}$$

By substituting these boundary conditions in (23), the state at the measurement point is reduced to

$$X(z_0) = \begin{bmatrix} G_1 \\ G_2 \end{bmatrix} P(0), \tag{26}$$

where

$$\begin{bmatrix} G_1 \\ G_2 \end{bmatrix} = \frac{1}{2}\left(M^{\ell_0} \begin{bmatrix} 1 \\ -\frac{t_{21}}{t_{22}} \end{bmatrix} + (\mathcal{S}^{\ell_2,\ell_1})^{-1} \begin{bmatrix} \frac{1}{t_{22}} \\ 0 \end{bmatrix} \right) \tag{27}$$

is the transfer matrix that characterizes the dynamic behavior of the wave at the measurement point z_0 for any source $P(0)$.

3.1 Transfer Function G_1

Since only the pressure $P(z_0)$ is measured for fault location, the following study focuses on the relationship given by

$$P(z_0) = G_1 P(0). \tag{28}$$

Thus, the properties of the transfer function G_1 are analyzed in terms of the pipeline parameters and the specific type of fault. By substituting the specific expressions for coefficients t_{ij} and after algebraically simplifying, the transfer function G_1 can be written as

$$G_1 = \frac{e^{\frac{-\ell_0}{c}\tilde{\gamma}} + R_f e^{\frac{-\ell_0-2\ell_1}{c}\tilde{\gamma}} + T_f^2 e^{\frac{-\ell_0-2\ell_1}{c}\tilde{\gamma}} \left(\frac{e^{\frac{-2\ell_2}{c}\tilde{\gamma}}}{1-R_f e^{\frac{-2\ell_2}{c}\tilde{\gamma}}} \right)}{1 + R_f e^{\frac{-2\ell_0-2\ell_1}{c}\tilde{\gamma}} + T_f^2 e^{\frac{-2\ell_0-2\ell_1}{c}\tilde{\gamma}} \left(\frac{e^{\frac{-2\ell_2}{c}\tilde{\gamma}}}{1-R_f e^{\frac{-2\ell_2}{c}\tilde{\gamma}}} \right)}, \tag{29}$$

with the reflection and transmission coefficient R_f and T_f for the respective fault $f = l$ or b and distances ℓ_i for $i = 0, 1, 2$. As shown in Fig. 6, the exponential functions $g_i(s) = e^{\frac{-\ell_i}{c}\tilde{\gamma}(s)}$ have a clear interpretation as a delay for low frequencies. Moreover, the fault effects are simpler to interpret through reflection and transmission parameters for a wave propagation study than through the impedances F_l^* and F_b^*.

Peralta and Verde (2021) proved that the graph $\mathcal{G}_1$ shown in Fig. 7 is equivalent to (29) with the input vertex $v_8 = P(0)$ and the output $v_9 = P(z_0)$. In other words, $\mathcal{G}_1$ describes the expansion of (29) and is the starting point for the wave propagation analysis in fault conditions.

The graph consists of 9 vertices and 12 transmittances of type, R_f, T_f and $g_i(s) = e^{\frac{-\ell_i}{c}\tilde{\gamma}}$ for $i = 0, 1, 2$. Note that the inverse transform of $g_i(s)$ acts as a time delay $t_i = \ell_i/c$ with an attenuation factor, which depends on the propagation function $\gamma(s)$.

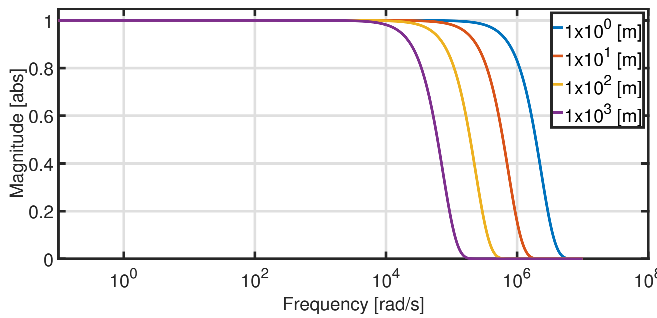

Figure 6. Gain of function $g_i(s)$ for different lengths l_i in air at 20°C as a propagation medium

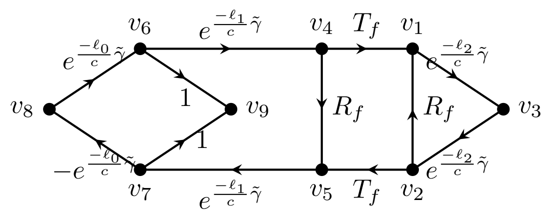

Figure 7. Equivalent graph $\mathcal{G}_1$ for a pipe with a fault

4. IDENTIFICATION OF FAULT BY MEANS OF REFLECTION COEFFICIENT

If an intact pipe is considered, then $R_f = 0$, $T_f = 1$, and the vertex $v_9 = P(z_0)$ is the pressure at the measurement point. One identifies two paths in $\mathcal{G}_1$. One travels from the source v_8 by $v_6 \to v_9$ in the positive direction with a time delay of ℓ_0/c. The other path starts in v_8 and arrives to $v_3 = P(L)$, returning by the path $v_3 \to v_2 \to v_5 \to v_7 \to v_9$ after a time of $(2L - \ell_0)/c$. After this time, the signal consists of reflexed waves. Thus, the signal at v_9 arriving from v_6 or v_7 is only suitable for a fault location during the time window $TW = (2L - \ell_0)/c$. The rest of the transient response is an overlapping of wave signals that are not easy to recognize.

4.1 Wave Pattern Features with a Fault

One can recognize the pattern response of v_9 for $t < TW$ as response to the impulse $v_8 = p(0, t) = \delta(t)$ from the following simple paths and their transmittances.

Path 1: The source signal $\delta(t)$ traveling by the simple path $v_8 \to v_6 \to v_9$ arrives at v_9 with negligible attenuation in a time $\tau_0 = \ell_0/c$. In other words, its effect is the impulse $p(z_0, \tau_0) = \delta(t - \ell_0/c)$.

Path 2: From v_8, the source travels, and part of the signal is reflected by the simple path

$$v_8 \to v_6 \to v_4 \to v_5 \to v_7 \to v_9$$

arriving at v_9 in time $\tau_f = 2\ell_1/c + \tau_0$ with an attenuated factor given by R_f. Therefore, $p(z_0, \tau_f) = R_f \delta(t - \tau_f)$ with $\tau_f < TW$, and the fault position can be determined by $\ell_1 = c(\tau_f - \tau_0)/2$.

Path 3: Another simple path of the signal leaving v_8 is

$$v_8 \to v_6 \to v_4 \to v_1 \to v_3 \to v_2 \to v_5 \to v_7 \to v_9.$$

 Copyright©AMCA. Todos los Derechos Reservados www.amca.mx

Through this path, the signal arrives at v_9 in a time $TW > \tau_f$ after its departure.

The above 3 paths are the only simple ones in $\mathcal{G}_1$. Path 2 is critical for fault diagnosis since it characterizes the damage type, its magnitude and position. The rest of the possible paths in the graph are not simple and can generate multiple waves in v_9. By considering the paths that pass only twice through v_8, one identifies the following.

Path 4: The source $\delta(t)$ travels by path

$$v_8 \to v_6 \to v_4 \to v_5 \to v_7 \to v_8 \to v_6 \to v_9$$

and arrives at v_9 in a time $\tau_2 = \tau_f + 2\tau_0$, passing twice by $v_8 \to v_6$. Note that the signal effect on v_9 allows the verification of the fault in some cases since the response is $-R_f\delta(t-\tau_2)$ with $\tau_2 > \tau_f$.

Path 5: According to path 4, the signal travels until v_6 and continues by $v_4 \to v_5 \to v_7 \to v_9$ until also arriving at v_9 but in a time $\tau_3 = 2\tau_f + \tau_0$.

Path 6: A signal that now passes through the vertex v_6 three times arrives at v_9 in time $\tau_4 = 2\tau_f + 3\tau_0$.

Thus, the wave traveling along path 2 allows the detection of the position ℓ_1 for both faults and corresponds to the second signal arriving at the vertex v_9 since $\tau_0 < \tau_f < TW$. To estimate the reflection factor and type of fault, the impulse response amplitude at time τ_f is proposed because the magnitude of the exponential functions $e^{\frac{-\ell_i}{c}\tilde{\gamma}(s)}$ is equal to 1 at low frequencies and for short distances. Note that the impulse is positive for a partial blockage and is negative for a leakage. One can also say that if $\ell_2 \to \infty$, $TW \to \infty$; furthermore, there is no reflected wave generated by the end. As a consequence, the patterns for fault diagnosis can be formally established by **Fact 1**.

Fact 1: *Consider the graph $\mathcal{G}_1$ with $\delta_v = 0$ that is associated with the fault diagnosis system of Fig. 1 and the impulse source $v_8 = P(0,t) = \delta(t)$. Thus, according to the previous graph analysis, the transient response or pressure pattern $v_9 = p(z_0, t)$ measured at z_0 is described by the impulse set*

$$A_0\delta(t-\tau_0)+A_f\delta(t-\tau_f)+A_{TW}\delta(t-TW)+\sum_{i=2}^{\infty}A_i\delta(t-\tau_i),$$

where magnitudes and delays of the impulses are related to the damage conditions. For an intact line and a line that has a leak or a blockage at some points of the line, the patterns are characterized by their respective relevant features.

(1) For an intact pipe, the impulse response has the magnitudes $A_0 = A_{TW} = 1$ with known time delays $\tau_0 = \ell_0/c$ and $TW = (2L-\ell_0)/c$; the rest of the impulses for $TW > \tau_i$ have magnitude 0.

(2) For a pipe with a leak or a partial blockage, only the second impulse gives information of the fault with known $A_0 = 1$ and τ_0. The reflection coefficient is given by $R_f = A_f$, and the rest of the impulses could be overlapped without explicit information of the fault. The delay τ_f allows the estimation of the distance of the fault to z_0 from the relation $\ell_1 = c(\tau_f - \tau_0)/2$. Moreover, the second impulse is negative for a leak and is positive for a blockage.

5. IMPULSE RESPONSE PROPAGATION TESTS

To show the simplicity of the diagnosis by using the features given in **Fact 1**, a pipeline with a fault and parameters given in Table 1 is considered. The system is simulated by using the Simulink toolbox (MATLAB, 2021) with a measurement point at $z_0 = 1$ m and a leak and a partial blockage at $z_1 = 4$ m or equivalently at a distance $\ell_1 = z_1 - z_0 = 3$ m from the measurement point. On the other hand, the generation of the excitation wave in a real device is a fundamental aspect for obtaining reliable results. Since the signal shape must be generated by the response from a loudspeaker, Delgado (2021) characterized a loudspeaker, where from the experiments carried out with the sound source in the form of a pulse, it was considered convenient to generate a short and smooth signal (in a mathematical sense) in order to get a pulse in the microphone. Therefore, it was proposed to generate the exponential function

$$p(0,t) = \exp\left(-(t-\tau)^2/2\sigma^2\right) \tag{30}$$

with values $\sigma = 0.1$ ms and $\tau = 2.2604$ ms. Through the value of σ is possible to choose the time in which the signal excites the system. For the selection of a short signal, a duration of approximately 0.5 ms was considered.

Table 1. Pipeline parameters for the diagnosis test on air at 20°C as a propagation medium

$c = 343$ m/s	$\rho_0 = 1.21$ kg/m^3
$\phi = 0.077$ m	$L = 10$ m
$F_l^* = 98,100$ Pa·s/m^3	$F_b^* = 784,800$ Pa·s/m^3

The pressure evolution $p(z_0, t)$ is shown in Figs. 8 and 9 for a leak and a blockage, respectively. From the set of impulses, one can identify in both responses that the results are coherent with the features established in **Fact 1**.

(1) The first pulse arrives at the measurement point in $\tau_0 \approx 5.176$ ms and the second one at $\tau_f \approx 22.67$ ms; therefore, according to the second point of Fact 1, the distance from the fault to measurement point is then $\ell_1 \approx 3$ m or equivalently $z_1 = 4$ m.

(2) The amplitude of the second pulse is $A_f = -0.318 \approx R_l$ for the leak and $A_f = 0.8108 \approx R_b$ for the blockage; thus, through the results given by Figs. 3 and 4, one obtains that $F_l^* \approx 121,036$ and $F_b^* \approx 789,000$ Pa·s/m^3.

As a result, the diagnostic for the two simulated scenarios coincides with the established conditions in **Fact 1**.

 Copyright©AMCA. Todos los Derechos Reservados www.amca.mx

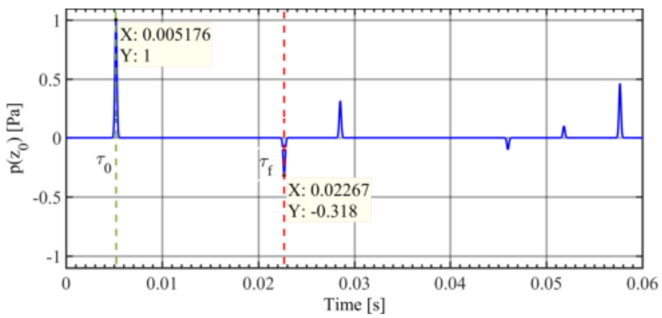

Figure 8. Evolution of the pressure at $z_0 = 1$ m and a leak located at $z_1 = 4$ m

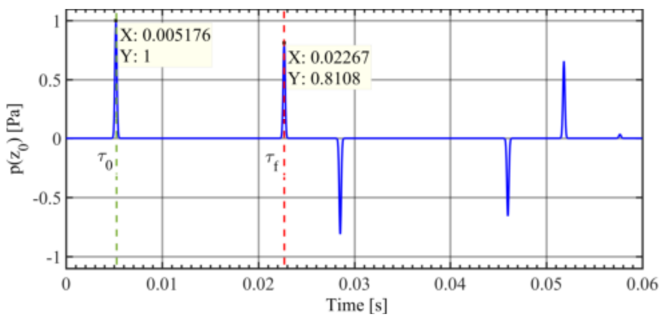

Figure 9. Evolution of the pressure at $z_0 = 1$ m and a blockage located at $z_1 = 4$ m

6. CONCLUSIONS

This work introduced a study of the effects of acoustic wave propagation in a pipe with absorption under fault conditions. By expressing the model of infinite dimension with faults as a transfer matrix with transcendental functions using an oriented graph and considering an impulse and a single measurement point of the wave pressure as an external source, it allowed obtaining the fault parameter through the reflection coefficient for a blockage and a leak. An important remark from the analysis is the characterization of the time window TW in which the fault parameters can be easily identified from the transient response. The rest of the transient response is a set of overlapped waves that are difficult to associate with fault features. Simulation results by MATLAB validated the proposed patterns for a leak and a blockage. Thus, it has been possible to perform a systematic analysis of the pipeline with damage, including the case of two faults.

REFERENCES

Blackstock, D. (2000). *Fundamentals of physical acoustics*. John Wiley and Sons.

Capponi, C., Ferrante, M., Zecchin, A.C., and Gong, J. (2017). Leak Detection in a Branched System by Inverse Transient Analysis with the Admittance Matrix Method. *Water Resour. Manag.*, 31(13), 4075–4089. doi:10.1007/s11269-017-1730-6.

Chaudhry, M.H. (2013). *Applied Hydraulic Transients*. SpringerLink: Bücher. Springer Science & Business Media, 3rd edition.

Datta, S. and Sarkar, S. (2016). A review on different pipeline fault detection methods. *J. Loss Prev. Process Ind.*, 41, 97–106. doi:10.1016/j.jlp.2016.03.010. URL `http://dx.doi.org/10.1016/j.jlp.2016.03.010`.

Delgado, F. (2021). *Diagnosticador acústico de fallas en ductos*. Master's thesis, Universidad Nacional Autónoma de México.

Farmer, E.J. (2017). *Detecting Leaks in Pipelines*. ISA.

Lee, P.J., Vítkovský, J.P., Lambert, M.F., Simpson, A.R., and Liggett, J.A. (2005). Leak location using the pattern of the frequency response diagram in pipelines: A numerical study. *Journal of Sound and Vibration*, 284(3-5), 1051–1073. doi:10.1016/j.jsv.2004.07.023.

Lu, H. and Iseley, T. (2018). Leakage detection techniques for oil and gas pipelines: State of the art. *Tunn. and Underground Space Technol.*, 98(September 2019), 344–350. doi:10.1038/cddis.2014.350.

MATLAB (2021). Matlab version 9.10.0.102886 (r2021a).

Meniconi, S., Brunone, B., Ferrante, M., and Capponi, C. (2016). Mechanism of interaction of pressure waves at a discrete partial blockage. *J. Fluids Struct.*, 62, 33–45. doi:10.1016/j.jfluidstructs.2015.12.010.

Mpesha, W., Gassman, S., and Chaudhry, H. (2001). Leak Detection in Pipes by frequency Response Method. *J. Hydraul. Eng.*, 127(2), 134–147.

Murvay, P.S.S. and Silea, I. (????). A survey on gas leak detection and localization techniques. *J. Loss Prev. Process Ind.*, (6), 966–973. doi: 10.1016/j.jlp.2012.05.010.

Peralta, J.A. and Verde, C. (2021). Signal patterns for fault detection by graph theory in pipelines. Manuscript submitted for publication.

Rubio Scola, I., Besanccon, G., and Didier, G. (2015). Frequency-model-based obstruction detection and location in a pipeline by output error minimization. In *IFAC SAFEPROCESS 2015*, volume 2, 232–237. doi: 10.1016/j.ifacol.2015.09.533.

Sattar, A. and Chaudhry, M. (2008). Leak detection in pipelines by frequency response method. *J. Hydraul. Res.*, 26(1), 138–151.

Sharp, D.B. and Campbell, D.M. (1997). Leak detection in pipes using acoustic pulse reflectometry. *Acustica*, 83(3), 560–566.

Wang, X., Camino, G.A., Che, T.C., and Ghidaoui, M.S. (2021). Factorized wave propagation model in tree-type pipe networks and its application to leak localization. *Mech. Syst. Signal Process.*, 147(37), 107116.

Zecchin, A.C., White, L.B., Lambert, M.F., and Simpson, A.R. (2005). Frequency – domain hypothesis testing approach to leak detection in a single fluid line. *Conference on Computing and Control for the Water Industry (CCWI) 2005 water management for the 21st century*, (2), 149–154.

 Copyright©AMCA. Todos los Derechos Reservados www.amca.mx